

# Point spread function and long-term stability of the H.E.S.S. reflectors

R. Cornils\*, S. Gillessen<sup>†</sup>, I. Jung<sup>†</sup>, W. Hofmann<sup>†</sup>, G. Heinzelmann\* and the H.E.S.S. collaboration\*\*

\**Universität Hamburg, Institut für Experimentalphysik, Luruper Chaussee 149, D-22761 Hamburg, Germany*

<sup>†</sup>*Max-Planck-Institut für Kernphysik, PO Box 10 39 80, D-69029 Heidelberg, Germany*

\*\**<http://www.mpi-hd.mpg.de/hfm/HESS/HESS.html>*

**Abstract.** The 107 m<sup>2</sup> reflector of each H.E.S.S. telescope consists of 380 mirror facets with 60 cm diameter. Mirror facets are aligned by a fully automated system using stars imaged onto the lid of the Cherenkov camera. The alignment procedure, implying the automatic analysis of CCD images and control of the mirror actuators, has been proven to work reliably. On-axis, 80% of the reflected light is contained in a circle of less than 1 mrad (0.057° or 1.5 cm in the focal plane) diameter, well below specifications. The widening of the spot with increasing angle to the optical axis is in accordance with the expected behaviour based on simulations, and variations of spot size with elevation are uncritical. Deterioration of the point spread function over time is of no concern; recurrent monitoring over years proved the width to be stable and thus the support structure to be very stiff.

## INTRODUCTION

H.E.S.S. is a stereoscopic system of four large imaging atmospheric Cherenkov telescopes in the Khomas Highland of Namibia [1]. Each telescope has a tessellated reflector of 107 m<sup>2</sup> consisting of 380 round mirror facets with 60 cm diameter made of glass. Given the large number of mirror facets a fully automated alignment system has been developed, including motorized mirror supports, compact dedicated control electronics, and various algorithms and software tools [2, 3, 4, 5, 6].

The basic technique to align the mirror facets is illustrated in Fig. 1. The telescope is pointed towards an appropriate star whereupon all mirror facets generate individual images of the alignment star in the focal plane (closed lid of the Cherenkov camera). Actuator movements change the location of the corresponding image which is observed by a CCD camera at the center of the dish. Individual mirror facets are adjusted such that all star images are combined into a single spot at the center of the Cherenkov camera.

It is – to our knowledge – the first time that such a technique is used to align the mirrors of Cherenkov telescopes. The major advantages of this approach are evident: The alignment utilizes direct imaging in the focal plane using a natural point-like source at infinite distance, and it can be performed at the optimum elevation angle so that the effect of gravity-induced deformations of the support structure on the point spread function is minimized.

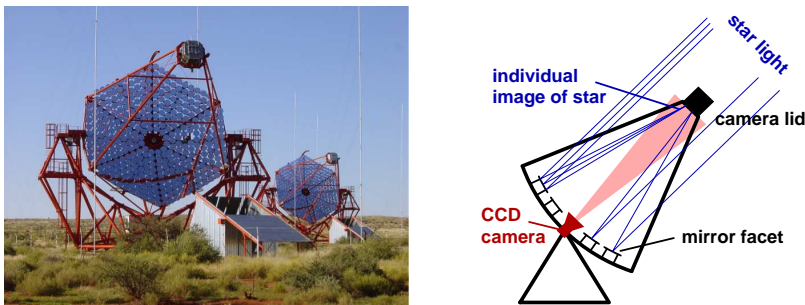


**FIGURE 1.** *Left:* The first two H.E.S.S. telescopes. *Right:* Mirror alignment technique.

## POINT SPREAD FUNCTION

Fig. 2 (left) shows a CCD image of the image of a star on the camera lid after the alignment of all mirror facets in relation to the size of a PMT pixel ( $0.16^\circ$  diameter). The intensity distribution represents the on-axis point spread function for telescope elevations within the range used for the alignment ( $55^\circ$ – $75^\circ$ ). The distribution is symmetrical without pronounced substructure and the width of the spot is well below the pixel size.

To parameterize the width of the intensity distributions, different quantities are used: the rms width  $\sigma_{proj}$  of the projected (1-dimensional) distributions and the radius  $r_{80\%}$  of a circle around the center of gravity of the image, containing 80% of the total intensity. Tab. 1 (top section) summarizes the on-axis widths of the point spread function around  $65^\circ$  elevation (mean alignment angle) of all four reflectors after their initial alignment. All values remain below the specification by a factor of more than two which demonstrates the excellent average mirror quality and accuracy of the alignment process. Remarkably,  $r_{80\%}$  for the whole reflector (containing spherical aberrations caused by outer mirrors) is even below the requirement for single (on-axis) mirror facets, 0.5 mrad.

### Variation of the point spread function across the field of view

Optical aberrations are significant in Cherenkov telescopes due to their single-mirror design (lack of corrective elements) and their modest  $f/a$  ratios. At some distance from the optical axis, the width of the point spread function is therefore expected to grow linearly with the angle  $\theta$  to the optical axis. For elevation angles around  $65^\circ$ , where the mirror facets were aligned, Fig. 2 (right) summarizes the spot parameters as a function of the angle  $\theta$ . Besides  $r_{80\%}$ , the rms widths of the distributions projected on the radial ( $\sigma_{radial}$ ) and tangential ( $\sigma_{tangential}$ ) directions are given. The measurements demonstrate that the spot width primarily depends on  $\theta$ ; no other systematic trend has been found.

To verify that the measured intensity distribution is quantitatively understood, Monte Carlo simulations of the actual optical system were performed, including the exact locations of all mirrors, the measured average spot size of the mirror facets, and the simulated precision of the alignment algorithm. The results are included in Fig. 2

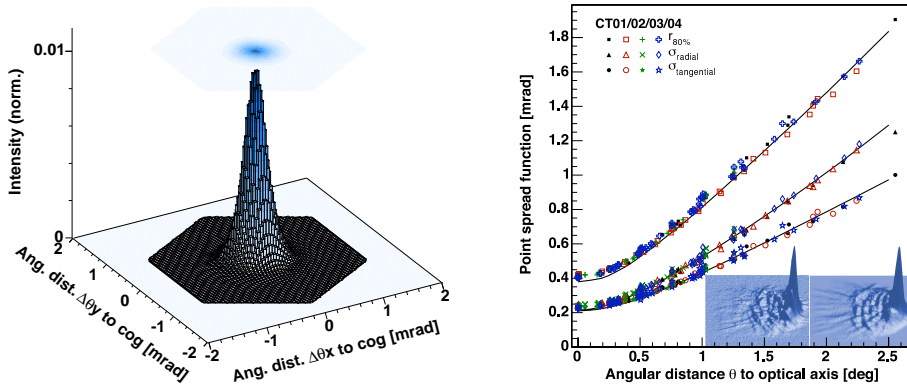


**FIGURE 2.** *Left:* On-axis intensity distribution of a star image on the camera lid (CT04). The hexagonal border indicates the size of a photomultiplier pixel, the boxes correspond to CCD image pixels. *Right:* Off-axis behaviour of the point spread function. *Right inset:* Measured spot shape (left, CT04) in comparison with a Monte Carlo generated image (right) at 2.3° off axis (image dimensions: 0.4° × 0.4°).

(right) as solid lines. Apart from a small deviation ( $\sim 5\%$  for  $r_{80\%}$ ) near the optical axis agreement is very good. This does not only include the width of the point spread function but also sub-structural details (knots and ribs) in the tails of the intensity distributions as demonstrated in Fig. 2 (right inset).

To describe the point spread function as a function of the angular distance  $\theta$  to the optical axis around the mean alignment elevation of 65° the parameterization

$$r_{80\%}(\theta) = (r_{\theta}^2 + d_{\theta}^2 \theta^2)^{1/2} \quad (1)$$

is used.  $r_{\theta}$  represents the on-axis width of the point spread function and  $d_{\theta}$  the increase of the width per degree angular distance to the optical axis. Fit parameters for the measured and simulated light spots are listed in Tab. 1 (middle section).

## Gravity-induced deformations of the telescope structure

Due to gravity-induced deformations of the support structure the spot is expected to widen outside the range of elevations where mirror facets are aligned. It is, however, hard to deduce what kind of deformations are responsible for the widening of the spot from measurements of the point spread function alone. A special operation mode was therefore implemented into the alignment system which allows for a detailed study of the deformation of the support structure: Rather than combining all individual spots to a uniform main spot, the spots can be arranged in arbitrary patterns.

Fig. 3 (left) shows the spots corresponding to individual mirror facets arranged in the form of a square matrix; each element of the matrix is the image generated by one mirror. By taking matrix images at different elevations, the deflection of mirror facets – and therefore the deformation of the dish – can be inferred from the relative movement

**TABLE 1.** Parameters of the point spread function. *Top section:* Measured on-axis point spread function. *Middle section:* Fit parameters for the description of the point spread function as a function of the angular distance  $\theta$  to the optical axis around  $65^\circ$  elevation. *Bottom section:* Fit parameters for the description of the on-axis point spread function as a function of the telescope elevation  $\Theta$ .

parameter	CT01	CT02	CT03	CT04	simulations	specifications
$\sigma_{proj}$ [mrad]	0.23	0.23	0.23	0.23	0.21	$\leq 0.50$
$r_{80\%}$ [mrad]	0.40	0.41	0.40	0.40	0.38	$\leq 0.90$
$r_\theta$ [mrad]	0.41	0.42	0.41	0.42	0.38	
$d_\theta$ [mrad deg $^{-1}$ ]	0.73	0.70	0.75	0.73	0.72	
$r_\Theta$ [mrad]	0.41	0.42	0.41	0.41		
$d_\Theta$ [mrad]	1.11	0.98	0.97	1.12		
$\Theta_c$ [deg]	60.7	62.5	66.5	64.6		

of the corresponding spots. As an example, Fig. 3 (right) shows the deflection of the mirror facets at  $29^\circ$  elevation with respect to  $65^\circ$ . Deformations are particularly strong at locations where the camera arms are attached and the dish is supported (shaded regions).

## Variation of the point spread function with telescope pointing

Fig. 4 (left) illustrates how the spot widths  $r_{80\%}$ ,  $\sigma_{azimuthal}$ , and  $\sigma_{altitudinal}$  change with telescope elevation  $\Theta$ . At fixed elevation, no significant dependence of the point spread function on telescope azimuth was observed. For elevations most relevant for observations, i.e. above  $45^\circ$ , the spot size  $r_{80\%}$  varies by less than 10%. At  $30^\circ$  it is about 40% larger than the minimum size but still well below the size of the PMT pixels. In addition, all reflectors behave almost identical.

The (on-axis) point spread function as a function of telescope elevation  $\Theta$  can be to a good approximation described by

$$r_{80\%}(\Theta) = (r_\Theta^2 + d_\Theta^2 (\sin \Theta - \sin \Theta_c)^2)^{1/2} \quad (2)$$

where  $r_\Theta$  is the minimum of the width and  $\Theta_c$  its location in elevation;  $d_\Theta$  specifies the increase of the width per  $90^\circ$  elevation. Values for all four reflectors are listed in Tab. 1 (bottom section).

## Long-term stability of the point spread function

Measurements of the initial status of all reflectors were performed right after their respective alignment and prior to the installation of the Cherenkov cameras. The increase in spot size due to the installation of the cameras remained below 30% in  $r_{80\%}$  for all telescopes, which is uncritical. This may be caused by differences in the weight of the camera as compared to the dummy weight used during initial alignment and a small offset between the position of the camera focal plane and of the alignment screen.

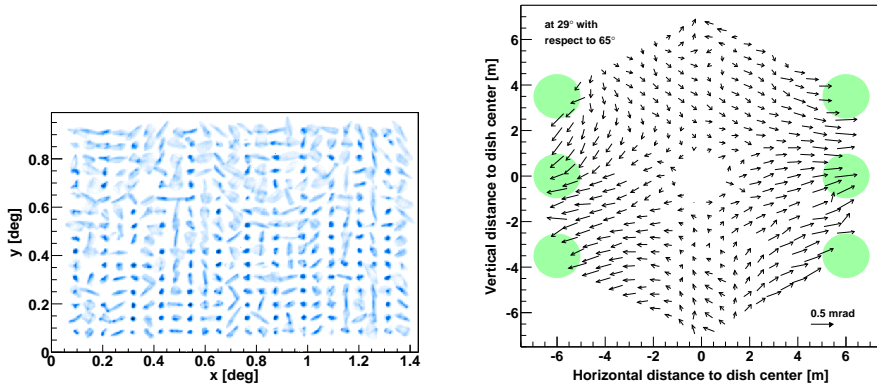


**FIGURE 3.** *Left:* Spot matrix: Each star image corresponds to an individual mirror facet at a certain location in the dish (facets of CT03). *Right:* Mirror deflections at  $29^\circ$  elevation with respect to  $65^\circ$  (CT03, arrows scaled by the square root of the deflection).

A critical issue is the stability of the point spread function over time. The alignment of the mirror facets of the first telescope (CT03) was completed in February 2002; no realignment has been performed since then. However, recurrent measurements of the on-axis point spread function with varying elevation have been carried out to monitor the quality of the alignment. For every set of measurements a fit according to Eqn. 2 was performed and the value of  $r_{80\%}(65^\circ)$  then calculated. The evolution of this parameter with time is shown in Fig. 4 (right). Only a small increase of 0.024 mrad or 6% per year is observed indicating an outstanding long-term stability of the telescope structure. This is in contrast to initial expectations which predicted realignments to be required at least once per year. The time base for measurements of other telescopes is as yet too small to draw a final conclusion, but recent results for the second telescope (CT02, Fig. 4 (right)) look very promising. It might indeed turn out that a realignment will not be necessary for the whole lifetime of the facets. However, the complete procedure for reproducibly resetting the point spread function to its optimum can be performed in a few hours.

## CONCLUSION

The alignment of the four H.E.S.S. reflectors was a proof of concept and a test of all technologies involved: mechanics, electronics, software, algorithms, and the alignment technique itself. All components work as expected, and the resulting point spread function significantly exceeds the requirements. The four reflectors behave very similar which demonstrates the high accuracy of the support structure and the reproducibility of the alignment process. This is complemented by an excellent long-term stability of the telescope structures; only a small increase in spot size is observed over a period of more than two years. To conclude: H.E.S.S. successfully pioneered star-based automated mirror alignments in air-Cherenkov astronomy.

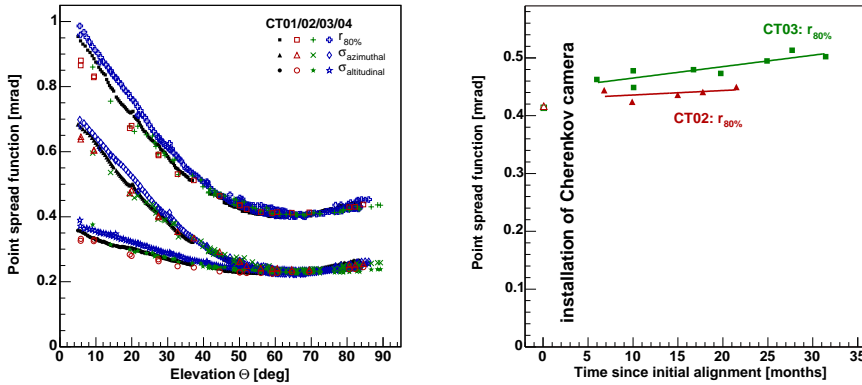


**FIGURE 4.** *Left:* Effect of the elevation-dependent deformation on the point spread function. *Right:* Evolution of the point spread function at  $65^\circ$  elevation for the first two H.E.S.S. telescopes.

## ACKNOWLEDGMENTS

The support of the Namibian authorities and of the University of Namibia in facilitating the construction and operation of H.E.S.S. is gratefully acknowledged, as is the support by the German Ministry for Education and Research (BMBF), the Max Planck Society, the French Ministry for Research, the CNRS-IN2P3 and the Astroparticle Interdisciplinary Programme of the CNRS, the U.K. Particle Physics and Astronomy Research Council (PPARC), the IPNP of the Charles University, the South African Department of Science and Technology and National Research Foundation, and by the University of Namibia. We appreciate the excellent work of the technical support staff in Berlin, Durham, Hamburg, Heidelberg, Palaiseau, Paris, Saclay, and in Namibia in the construction and operation of the equipment.

## REFERENCES

1. Hofmann, W., et al., “Status of the H.E.S.S. project,” in *Proc. 28th ICRC*, edited by T. Kajita, Y. Asaoka, A. Kawachi, et al., Universal Academy Press, Inc., 2003, vol. 5, pp. 2811–2814.
2. Cornils, R., and Jung, I., “Alignment of the mirror facets of the H.E.S.S. Cherenkov telescopes,” in *Proceedings of the 27th International Cosmic Ray Conference*, edited by M. Simon, E. Lorenz, and M. Pohl, Copernicus Gesellschaft, 2001, vol. 7, pp. 2879–2882.
3. Cornils, R., Gillessen, S., Jung, I., Hofmann, W., and Heinzelmann, G., “Mirror alignment and optical quality of the H.E.S.S. imaging atmospheric Cherenkov telescopes,” in *The Universe Viewed in Gamma-Rays*, edited by R. Enomoto, M. Mori, and S. Yanagita, Universal Academy Press, Inc., 2003, pp. 403–408.
4. Cornils, R., Gillessen, S., Jung, I., Hofmann, W., Heinzelmann, G., et al., “Mirror alignment and performance of the optical system of the H.E.S.S. imaging atmospheric Cherenkov telescopes,” in *Proceedings of the 28th International Cosmic Ray Conference*, edited by T. Kajita, Y. Asaoka, A. Kawachi, Y. Matsubara, and M. Sasaki, Universal Academy Press, Inc., 2003, vol. 5, pp. 2875–2878.
5. Bernlöhner, K., Carrol, O., Cornils, R., Elfaheem, S., et al., *Astroparticle Physics*, **20**, 111–128 (2003).
6. Cornils, R., Gillessen, S., Jung, I., Hofmann, W., et al., *Astroparticle Physics*, **20**, 129–143 (2003).